

Poly(3-alkylthiophenes) and polydiphenylamine copolymers: a comparative study using electrochemical impedance spectroscopy

Danielly Cristina Bento · Elaine Cristina Rodrigues Maia · Paulo Rogério Pinto Rodrigues · Gregory J. Moore · Guy Louarn · Henrique de Santana

Received: 8 July 2013 / Accepted: 23 August 2013 / Published online: 17 September 2013
© Springer Science+Business Media New York 2013

Abstract This study compares the electrical properties of two homopolymers, poly(3-methylthiophene) and poly(3-octylthiophene), and their copolymers with polydiphenylamine, previously synthesized electrochemically on a platinum wire electrode (average area 0.19 cm^2) in $0.100 \text{ mol L}^{-1} \text{ LiClO}_4$ at $18 \text{ }^\circ\text{C}$. Based on the cyclic voltammetry data from these systems, electrochemical impedance spectroscopy (EIS) was used to evaluate the resistive and capacitive properties of the homo- and copolymers using the open-circuit potential (OCP) and overvoltage potential methods. The copolymer of poly(3-methylthiophene) and polydiphenylamine showed lower resistivity between films obtained by OCP and overvoltage potential. For all EIS images obtained by overvoltage potential there was a drop in resistivity and lower variation among the capacitance values. Using a Bode plot, we observed two time constants related to the radical cation and dication species, as characterized by Raman spectroscopy. Using scanning electron microscopy, it was possible to observe the changes in the morphological structures of the copolymers by comparison with the homopolymers, confirming the

influence of greater active area on the improved conductivity of the copolymers.

1 Introduction

Considerable progress has been made in optoelectronics using poly(3-alkylthiophene)s (P3ATs) which have found applications in organic light-emitting diodes (OLED), organic solar cells, low-cost integrated circuits and organic field effect transistors (OFET) [1–6]. P3ATs are highly photosensitive, with sufficient light absorption to allow their use as optical absorbers in photovoltaic cells [3, 7, 8].

One significant characteristic of P3ATs is that they change from insulator to semiconductor by a process of oxidation or reduction of the conjugated π system [9–11]. This process induces a transition from aromatic to quinone form, allowing the formation of radical cation and dication segments in the polymer chain [12]. Redox reactions in the polymer semiconductors are responsible for the electrical conductivity, and also for the electrochemical and electrochromic properties of these materials.

Understanding the conductive process in organic polymer materials is extremely important, both for understanding the factors that influence their electronic properties and in terms of possible applications [13]. For characterizing semiconductor polymer materials electrochemical impedance spectroscopy (EIS) has been used in order to determine and understand the electrical properties over a broad band of frequencies [14].

EIS is one of the most widely used electrochemical analysis techniques. Various systems can be analyzed, including electrodes coated with electroactive polymer films, solutions containing immiscible liquids, ion-selective electrodes, electrodes coated with fine inorganic oxide films, etc. EIS provides information on the various time constants associated with the electrochemical processes

D. C. Bento · E. C. R. Maia · H. de Santana (✉)
Departamento de Química, Universidade Estadual de Londrina,
Londrina, PR 86051-990, Brazil
e-mail: hensan@uel.br

P. R. P. Rodrigues
Departamento de Química, Universidade Estadual Do Centro
Oeste, Guarapuava, PR 85040080, Brazil

G. J. Moore
Yardney Technical Products, Inc., East Greenwich, RI, USA

G. Louarn
Université de Nantes, CNRS, Institut Des Matériaux Jean Rouxel
IMN, F-44322 Nantes, France

that occur at the interfaces of an electrode. One of its main applications is in the study of electrodes coated with high-resistance films, characterized in terms of their electrical properties, such as film resistance and capacitance [15, 16].

This study presents an electrochemical synthesis of homopolymers poly(3-methylthiophene) (P3MT) and poly(3-octylthiophene) (P3OT) and their copolymers with Polydiphenylamine (PDPA). Chronoamperometry was used to synthesize the blended copolymers: P3MT and PDPA (CP3MT) and P3OT and PDPA (CP3OT) on platinum wire in LiClO_4 at 18 °C. The data obtained by cyclic voltammetry were used in conjunction with EIS. EIS was used to evaluate and compare the resistive and capacitive properties of homo- and copolymers by open-circuit potential (OCP) and overvoltage potential. The results obtained from the Bode plots were confirmed by Raman spectroscopy, and scanning electron microscopy (SEM) was used to verify changes in the morphologies of the homo- and copolymers; the morphology responsible for increasing the active area of the film surface.

2 Experimental section

2.1 Chemicals

The 3-methylthiophene ($\text{C}_5\text{H}_7\text{S}$) and 3-octylthiophene ($\text{C}_{12}\text{H}_2\text{S}$) monomers were used as received. The supporting electrolyte was 99 % pure lithium perchlorate (LiClO_4) supplied by Acros Organics. Acetonitrile (CH_3CN) was obtained from JT Baker, purity 99.5 %, HPLC grade. The diphenylamine ($(\text{C}_6\text{H}_5)_2\text{NH}$) supplied by Allkimia Ltda was recrystallized three times in petroleum ether supplied by Labsynth Ltda, 99.8 %.

2.2 Synthesis by chronoamperometry (CA) and investigation by cyclic voltammetry (CV)

A platinum wire electrode with a surface area of 0.19 cm^2 was used to synthesize the homo- and copolymers. All potentials were determined by reference to Ag/AgCl in a Luggin capillary and a 0.100 mol L^{-1} solution of LiClO_4 in acetonitrile ($\text{LiClO}_4/\text{ACN}$).

Table 1 gives the conditions at 18 °C under which the P3MT and P3OT copolymer films were synthesized. The copolymers were obtained by blending a 5:1 solution of monomers 3MT and DPA, denoted copolymer CP3MT, and of 3OCT and DPA, denoted copolymer CP3OT. After producing the films, they were immersed in acetonitrile to remove excess species of low molecular weight and excess electrolyte [4].

CA and CV curves were obtained using an Autolab PGSTAT 302 N potentiostat/galvanostat coupled to a microcomputer running NOVA 1.8.

2.3 Electrochemical impedance spectroscopy (EIS)

Impedance spectra were obtained using an Autolab PGSTAT 302 N potentiostat with FRAM32 impedance module and varying the frequency from 100 kHz to 0.01 Hz. The open-circuit stabilization potential (E_{OC}) was reached when E_{OC} remained constant ± 5 mV for 30 min. The applied perturbation voltage was ± 10 mV of E_{OC} .

2.4 Scanning electron microscopy (SEM)

For SEM analysis, the homo- and copolymers were deposited electrochemically at 18 °C in 0.100 mol L^{-1} $\text{LiClO}_4/\text{ACN}$ over indium-doped tin oxide (ITO) following the method used by de Santana et al. [4]. The images were obtained on a PHILIPS Quanta 200 (FEI) electron microscope at a voltage of 25 keV, beam-sample distance of 7.9–8.1 mm, image scale of 2.0–50.0 μm , at a magnification of 24000–30000X.

2.5 Spectroscopic characterization

Raman spectra were obtained using a DeltaNu Advantage532[®] portable Raman spectrometer, excited at 532 nm with resolution of 8 cm^{-1} . DeltaNu NuSpec software with baseline resources was used to remove background fluorescence.

3 Results and discussion

Table 2 gives the values of anodic potential (E_{ox}), potential variation range (ΔE) and overvoltage potential (η) of each system obtained from voltammograms and used in the EIS. The cyclic voltammograms of the homo- and copolymers deposited on the platinum wire reproduced those obtained from the films produced on platinum plates with higher surface area [1, 4].

Figure 1 shows the Nyquist plot of the homo- and copolymers on platinum in 0.100 mol L^{-1} $\text{LiClO}_4/\text{ACN}$ obtained at OCP. The Nyquist plot of the P3OT is highlighted in Fig. 1 as exhibiting the largest diameter semicircle.

We observed semicircle diameter variations corresponding to changes in the charge transfer resistances (R_{CT}) of the films [17]. The semicircles were not perfect and the imperfections could indicate possible frequency dependencies on conductivity and dielectric constant [14, 17–22].

Table 3 gives the values of maximum frequencies (f), charge R_{CT} and E_{OC} obtained for the films using OCP.

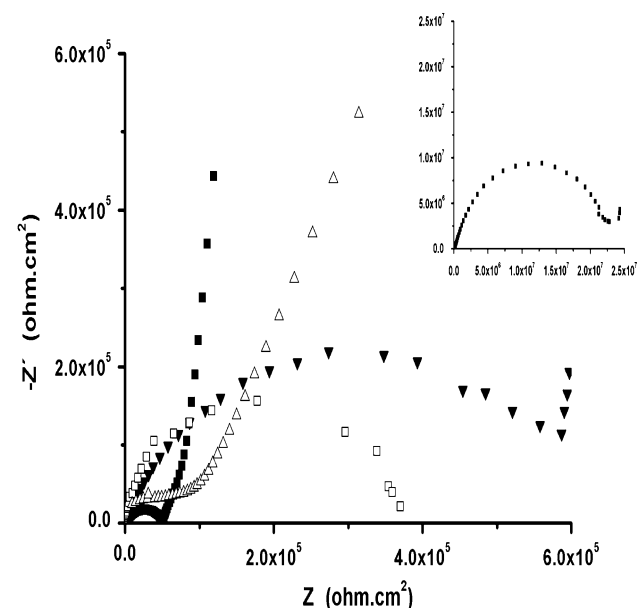
Values of R_{CT} rise in the following sequence: CP3MT < P3MT < CP3OT < P3OT. Bearing in mind that among the films obtained using OCP, the smallest diameter

Table 1 Chronoamperometry (CA) experimental conditions for synthesizing homo- and copolymers

Films	Concentration (mol L ⁻¹)		Time (s)	Applied potential (V vs. Ag/AgCl)	Current density (A cm ⁻²)
	DPA	3MT ou 3OT			
P3MT	–	0.035	240	1.70	6.05 × 10 ⁻⁶
P3OT	–	0.040	240	1.75	8.42 × 10 ⁻⁶
CP3MT	0.020	0.100	600	1.70	1.54 × 10 ⁻⁵
CP3OT	0.020	0.100	600	1.75	11.15 × 10 ⁻⁶

Table 2 Anodic potential (E_{ox}), potential variation range (ΔE) and overvoltage potential (η) values for each system determined by homo- and copolymers' CVs

Films	E_{ox} [V vs. Ag _(s) /AgCl _(s)]	ΔE [V vs. Ag _(s) /AgCl _(s)]	η (V vs. Ag _(s) /AgCl _(s))
P3MT	0.74	0.27:0.65:0.95:1.17:1.35	0.65 ± 0.10
P3OT	1.15	0.31:0.84:1.02:1.40:1.58	0.84 ± 0.10
CP3MT	1.00	0.42:0.65:0.77:1.00:1.00	0.65 ± 0.10
CP3OT	1.28	0.56:0.84:1.04:1.21:1.52	0.84 ± 0.10

**Fig. 1** Nyquist plots obtained by OCP for the following films deposited on a platinum plate in 0.100 mol L⁻¹ LiClO₄/ACN: (square) P3MT, (filled square) CP3MT, (triangle) P3OT and (filled inverted triangle) CP3OT. The highlight shows the P3OT semicircle

semicircle was for CP3MT, this film had the lowest resistivity. P3OT showed higher resistance (largest diameter semicircle), as can be seen in the highlight in Fig. 1 and is confirmed by the value of R_{CT} .

Figure 2 shows the Nyquist plot obtained at overvoltage potentials (η) for the homo- and copolymers on platinum in 0.100 mol L⁻¹ LiClO₄/ACN, as indicated in Table 2.

It is clear that when the overvoltage is applied all the semicircles produced show a better curvature than those

Table 3 Homo- and copolymers' values obtained per the nyquist plots using OCP for maximum frequency (f), charge transfer resistance (R_{CT}) and open-circuit potential (E_{OC})

Films	f (Hz)	R_{CT} (ohm.cm ²)	E_{OC} [V vs. Ag _(s) /AgCl _(s)]
P3MT	39.811	3.73 × 10 ⁵	0.591 ± 0.05
P3OT	0.3980	2.28 × 10 ⁷	0.604 ± 0.05
CP3MT	630.96	0.49 × 10 ⁵	0.458 ± 0.05
CP3OT	39.811	5.98 × 10 ⁵	0.539 ± 0.05

produced by OCP. Tolstopyatova et al. [23] observed that the resistive behavior of alkylthiophenes in the presence of overvoltage potential was dependent on the side chain polymers in the matrix. Similarly, the plots show that P3MT has a lower resistance than P3OT. The same applies to CP3MT by comparison with CP3OT.

Table 4 gives the values of maximum frequencies (f) and charge R_{CT} obtained by overvoltage potential.

As observed in the high-frequency region of the Nyquist plots, CP3MT has the lowest R_{CT} (Table 4) and for all EIS obtained at overvoltage potential, resistances were lower by comparison with those obtained at OCP. Bearing in mind that the overvoltage potential was chosen in the potential range in which the polymer is most conductive, this drop in R_{CT} is directly related to increased conductivity. This fact shows the importance of copolymerization on the behavior of these materials, since the chains of these polymers act as an alternate conductive pathway in resistive inorganic materials, causes a drop in the charge transfer resistance between particles and facilitates electron transport [24].

Figure 3 gives the Bode plots of the homo- and copolymers produced, together with the Nyquist plots, using overvoltage potential.

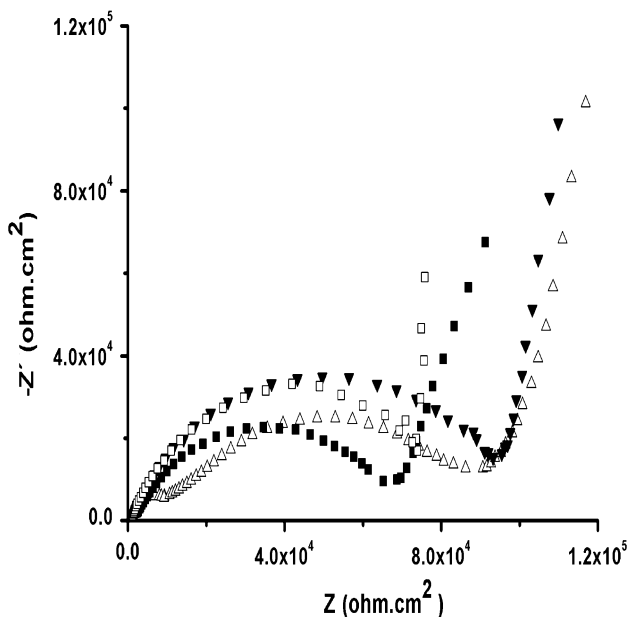


Fig. 2 Nyquist plots in 0.100 mol L⁻¹ LiClO₄/ACN, obtained at an overvoltage potential of 0.65 V for (square) P3MT and (filled square) CP3MT, and at 0.84 V for (triangle) P3OT and (filled inverted triangle) CP3OT

Table 4 Values obtain in the nyquist plots using overvoltage potential for homo- and copolymers for *f* and R_{CT}

Films	<i>f</i> (Hz)	R _{CT} (ohm.cm ²)
P3MT	199.53	7.81 × 10 ⁴
P3OT	398.22	7.91 × 10 ⁴
CP3MT	398.11	3.48 × 10 ⁴
CP3OT	199.53	9.18 × 10 ⁴

Analyzing the results in the Bode plots and the imperfect semicircles shown in the Nyquist plot (Fig. 2), we observed two time constants. This result could indicate that the process is occurring in two stages, and according to the literature [1, 4] they relate to oscillations of the radical cation and dication species in the polymer matrix.

Figure 4 gives the electrical double-layer capacitances (C_{DL}) based on the double-layer capacitance values (C) as a function of frequency (f). Values of C were determined based on the charge transfer resistance (R_{CT}) and relaxation frequency (f) obtained from the Nyquist plots for OCP and overvoltage (η), for the homo- and copolymers in LiClO₄/ACN, by applying Eq. 1 [25].

$$C = 1/2\pi f R_{CT} \tag{1}$$

Figure 4 gives the drop in capacitance with increasing frequency. In Fig. 4a and according to the Nyquist plot (Fig. 1), CP3MT has a lower resistance and higher capacitance; the greatest difference between P3MT and CP3MT was obtained for OCP and amounted to less than

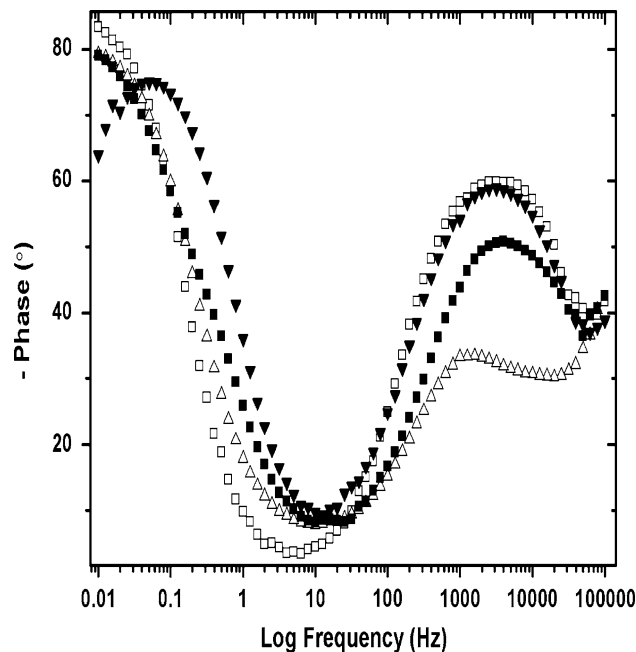


Fig. 3 Bode phase diagram in 0.100 mol L⁻¹ LiClO₄/ACN, obtained at an overvoltage potential of 0.65 V for (square) P3MT and (filled square) CP3MT, and at 0.84 V for (triangle) P3OT and (filled inverted triangle) CP3OT

30 Hz. CP3OT has a higher capacitance at low frequencies (up to 15 Hz) by comparison with its homopolymer [26]. The inset in Fig. 4a shows a better visualization of results. These results show that copolymerization induces increased conductivity for an open-circuit potential.

The capacitances obtained by overvoltage potential (Fig. 4b) do not show any significant differences in value for homo- and copolymers. This could be related to the application of an overvoltage potential, for both homo- and copolymers, within the range of potential in which the polymers show the highest conductivity.

Figure 5 gives the Raman spectra of the homo- and copolymers produced electrochemically in 0.100 mol L⁻¹ LiClO₄/ACN on a platinum wire electrode with a low surface area, and obtained at excitation radiation of 532 nm. We note that the Raman spectra were similar to those previously obtained for films deposited on platinum plates [1].

Table 5 lists the frequency values for the main spectral bands of the P3ATs and PDPA [4, 27]. The presence of frequencies at around 1,205, 1,322, 1,527 and 1,607 cm⁻¹ in the copolymer samples shows that radical cation segments of the PDPA are present in the copolymer matrix [27].

In the Raman spectra of copolymers CP3MT and CP3OT (Fig. 5), we observed a broadening of the bands at 1,450 and 1,453 cm⁻¹, assigned in Table 5 to the ν(C=C) symmetrical ring stretching, by comparison with homopolymers P3MT and P3OT. This stretching was used because it is sensitive to changes undergone by the aromatic ring in the

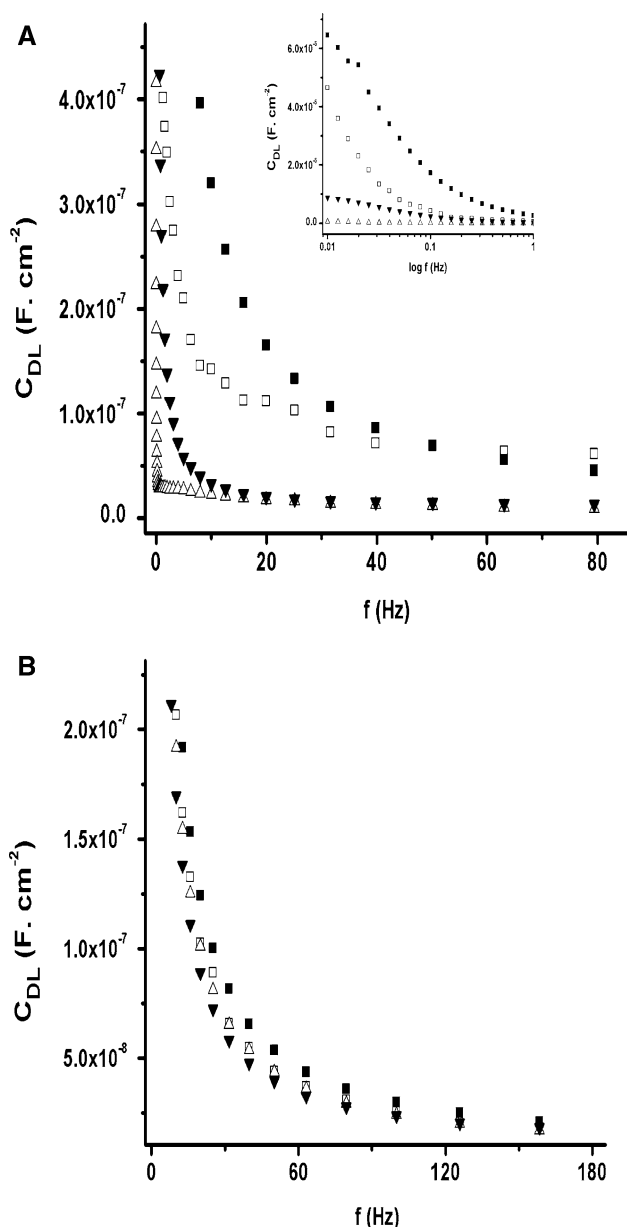


Fig. 4 Electrical double-layer capacitance (C_{DL}) as a function of frequency for homo- and copolymers in 0.100 M $\text{LiClO}_4/\text{ACN}$. **a** obtained at OCP and **b** at overvoltage potential of 0.65 V for (square) P3MT and (filled square) CP3MT, and at 0.84 V for (triangle) P3OT and (filled inverted triangle) CP3OT. The inset shows as a function of the log of frequency

presence of radical cation and dication segments in the matrix of polyalkylthiophenes. Deconvoluting the copolymer spectra, we observed three bands characteristic of radical cation, dication and aromatic segments with different relative intensities [1, 4, 28, 29].

In the deconvoluted spectrum of CP3OT, it was possible to observe an intense band for the dication segment, whereas in that of the CP3MT the radical cation band was most intense. This result has already been observed [1] and is due to the higher stabilization of the dication species in

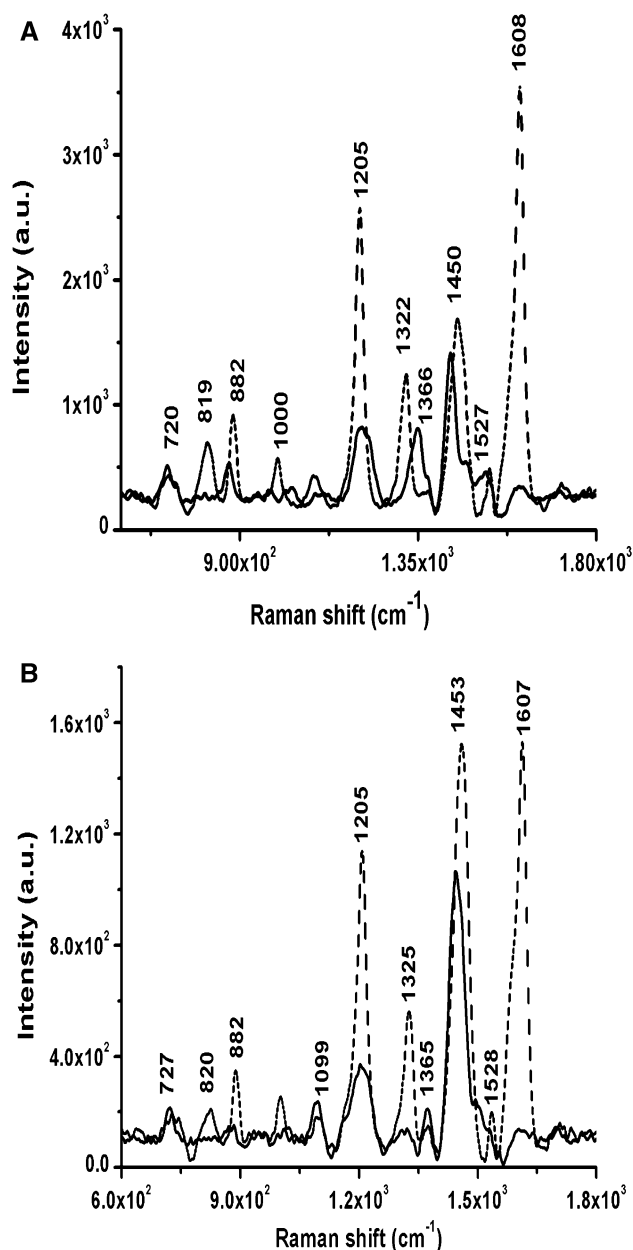


Fig. 5 Raman spectra of homo- (solid line) and copolymers (dotted line) as deposited on a platinum wire in 0.100 mol L^{-1} $\text{LiClO}_4/\text{ACN}$, **a** P3MT and CP3MT; **b** P3OT and CP3OT. $\lambda = 532$ nm

CP3OT and of the radical cation species in CP3MT, in contrast to what was observed in the deconvoluted spectra of the homopolymers, which showed higher intensity in the band attributed to the aromatic species [4]. The stabilization of the species in the film segments was already evident in the Bode plots (Fig. 3), showing that the process involves two stages.

Figure 6 shows SEM images of the homo- and copolymers obtained in 0.100 mol L^{-1} $\text{LiClO}_4/\text{ACN}$ on ITO.

Table 5 Characteristic Raman frequencies assigned to homo- and copolymers of P3ATs and PDPA

Raman frequencies (cm ⁻¹)					Assignment
P3MT	CP3MT	P3OT	CP3OT	PDPA	
984	1,000	1,094	1,099	–	$\nu^a(\text{C}-\text{C}_{\text{subst}})$
1,186	–	1,210	–	–	$\nu(\text{C}-\text{C}_{\text{inter ring}})$
–	1,205	–	1,205	1,205	$\beta^b(\text{C}-\text{H})$
–	1,322	–	1,325	1,324	$\nu(\text{C}-\text{C}_{\text{inter ring}})$
1,360	1,366	1,372	1,368	–	$\nu(\text{C}-\text{C}_{\text{ring}})$
1,454	1,450	1,450	1,453	–	$\nu(\text{C}=\text{C}_{\text{ring}})$
1,520	–	1,522	–	–	$\nu_{\text{as}}^c(\text{C}=\text{C}_{\text{ring}})$
–	1,527	–	1,528	1,525	$\nu(\text{C}-\text{N})$
–	1,608	–	1,607	1,609	$\nu(\text{C}=\text{C}_{\text{ring}})$

^a Symmetric stretching^b Bending mode^c Asymmetric stretching

Figure 6a, b shows that homopolymers are characterized by a more clustered and compact morphology, resulting in a material with a lower active area, whereas their

copolymers CP3MT and CP3OT (Fig. 6c, d) exhibit a more porous morphology, giving them a higher active area, with the result that these materials have a higher charge density, lower resistivity and greater capacitance [30].

4 Conclusions

The results presented above show that it might be possible to vary the charge density values of P3ATs by copolymerization with PDPA. EIS enabled us to determine the charge transfer resistance and capacitance values for all systems studied. The Bode plot shows two time constants related to the radical cation and dication species. The CP3MT copolymer exhibited lower resistivity between the films obtained by OCP and overvoltage potential. The P3OT film exhibited lower resistance, but copolymerization changed this property, increasing conductivity. For all EIS obtained using overvoltage potential, we observed a drop in resistivity and lower variation between capacitance values of homo- and copolymers.

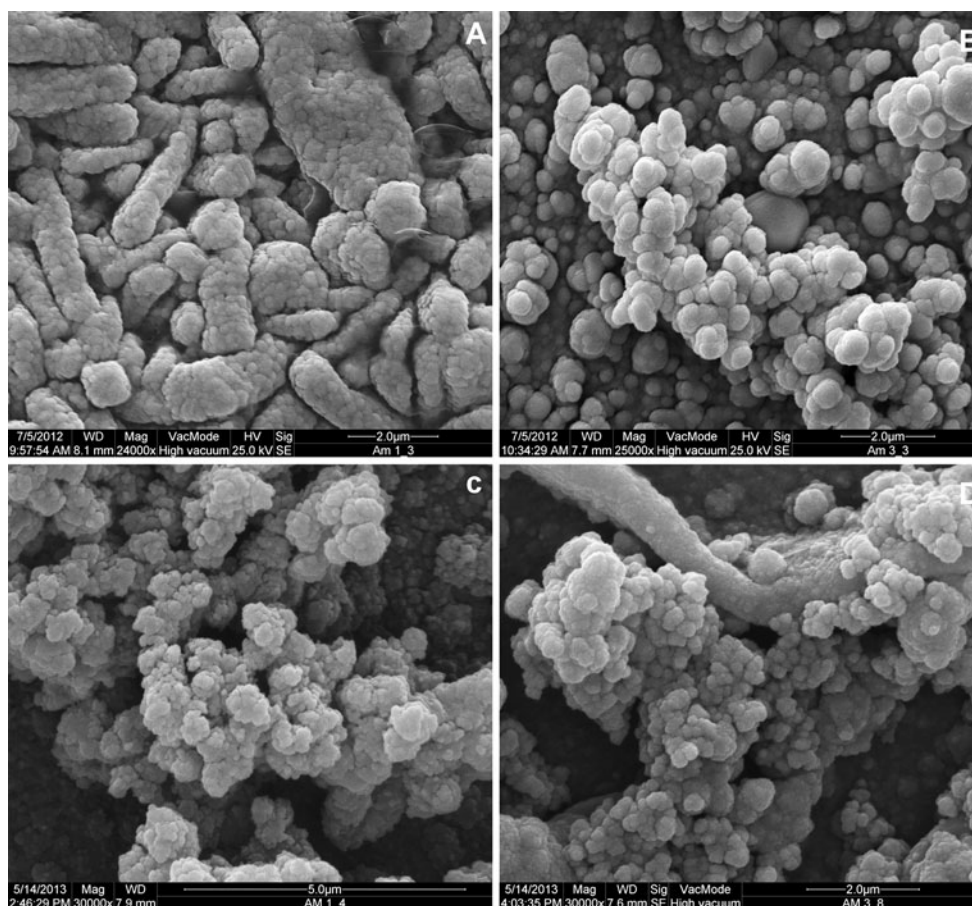


Fig. 6 Scanning electron microscopy images of homo- and copolymers deposited in 0.100 mol L⁻¹ LiClO₄/ACN on ITO: **a** P3MT, **b** P3OT, **c** CP3MT and **d** CP3OT

Raman spectroscopy enabled us to confirm and characterize the formation of the copolymers due to the simultaneous presence of the characteristic frequencies of P3ATs and PDPA. In the copolymer Raman spectra we observed that the radical cation segment was more stable than that of the homopolymers because of the contribution of the PDPA. Scanning electron microscopy enabled us to observe the morphological changes in the homo- and copolymers, confirming the influence of the more extensive active area on improvement of the copolymer conductivity.

Acknowledgments We would like to express our appreciation of the Spectroscopy Laboratory (SPEC) and Electron Microscopy and Microanalysis Laboratory (LMEM) at the PROPPG/Uel Multiuser Center, the Special Visiting Researcher Program (PVE) run by CAPES (Project n^o. 124/2012), and the Brazilian Research Centre (CNPq) and CAPES for their financial support.

References

- D.C. Bento, E.C.R. Maia, T.N.M. Cervantes, R.V. Fernandes, E. Di Mauro, E. Laureto, M.A.T. Da Silva, J.L. Duarte, I.F.L. Dias, H. De Santana, *Synth. Met.* **162**, 2433 (2012)
- F.M. Nodari, R.L. Patyk, L.S. Roman, A.R.V. Benvenho, I.A. Hummelgen, E.K.C. Yoshikawa, J. Gruber, *J. Mater. Sci.: Mater. Electron.* **21**, 1235 (2010)
- C.H. Kim, K. Kisie, J. Jung, J. Ulansk, D. Tondeliera, B. Geffroya, Y. Bonnassieuxa, G. Horowitza, *Synth. Met.* **162**, 460 (2012)
- H. De Santana, E. C. R. Maia, D. C. Bento, T. N. M. Cervantes, G. J. Moore, *J. Mater. Sci.: Mater. Electron.* (2013). doi:[10.1007/s10854-013-1254-7](https://doi.org/10.1007/s10854-013-1254-7)
- R. Singh, J. Kumar, R.K. Singh, A. Kaur, K.N. Sood, R.C. Rastogi, *Polymer* **46**, 9126 (2005)
- Z.J. Qi, W.D. Feng, Y.M. Sun, D.Z. Yan, Y.F. He, J. Yu, *J. Mater. Sci.: Mater. Electron.* **18**, 869 (2007)
- V.D. Mihailetchi, H.X. Xie, B. de Boer, L.J.A. Koster, P.W.M. Blom, *Adv. Funct. Mater.* **16**, 699 (2006)
- P. Vanlaeke, A. Swinnen, I. Haeldermans, G. Vanhoyland, T. Aernouts, D. Cheyys, C. Deibel, J. D'Haen, P. Heremans, J.S. Poortman, J. Manca, *Sol. Energy Mater. Sol. Cells* **90**, 2150 (2006)
- L.H.C. Mattoso, *Quim. Nova* **19**, 388 (1996)
- L. Micaroni, F.C. Nart, I.A. Hummelgen, *J. Solid State Electrochem.* **7**, 55 (2002)
- A. Ray, A.F. Richter, A.G. Macdiarmid, A. Epstein, *Synth. Met.* **29**, 151 (1989)
- E.S. Medeiros, J.E. Oliveira, N. Consolin-Filho, L.G. Paterno, L.H.C. Mattoso, *Electron. J. Mater. Processes (REMAP)* **7**(2), 62 (2012)
- A.G. Macdiarmid, *Synth. Met.* **125**, 11 (2001)
- E. Barsoukov, J.R. Macdonald, *Impedance spectroscopy: theory, experiment, and applications*, 2nd edn. (Wiley, New Jersey, 2005)
- E.M. Giroto, M.A. De Paoli, *Quim. Nova* **22**, 358 (1999)
- M. Tussolini, C. Spagnol, C.G. Everton, M.T. da Cunha, P.R.P. Rodrigues, *REM-Revista Escola de Minas* **60**. (2007)
- M. Tussolini, A. Viomar: A.L. Gallina, E.P. Banczek, M.T. Cunha, P.R.P. Rodrigues, *REM-Revista Escola de Minas* **66** (2013)
- Y. Li, J. Gao, G. Yu, Y. Cao, A.J. Heeger, *Chem. Phys. Lett.* **287**, 83 (1998)
- L.A. De Carvalho, A.R. De Andrade, P.R. Bueno, *Quim. Nova* **29**, 796 (2006)
- G.D. Sharma, D. Saxena, M.S. Roy, *Synth. Met.* **123**, 189 (2001)
- A. Janshoff, *Impedance spectroscopy* (Biophysical Chemistry Group, Johannes Gutenberg-Universität Mainz, Institut für Physikalische Chemie, Mainz, 2007)
- P.R.P. Rodrigues, I.V. Aoki, A.H.P. Andrade, E. Oliveira, S.M.L. Agostinho, *Br. Corros. J.* **31**, 305 (1996)
- E.G. Tolstopyatova, S.N. Sazonova, V.V. Malev, V.V. Kondratiev, *Electrochim. Acta* **50**, 1571 (2005)
- Y. Zhou, H. Xian, F. Li, S. Wu, Q. Lu, Y. Li, L. Wang, *Electrochim. Acta* **55**, 5905 (2010)
- E.G. Tolstopyatova, S.N. Sazonova, V.V. Kondratiev, V.V. Malev, *Russ. J. Electrochem.* **40**, 1073 (2004)
- S. Ebrahim, M. Soliman, T.M. Abdel-Fattah, *J. Electron. Mater.* **40**, 2033 (2011)
- H. De Santana, J.R.M.L.A. Matos, *Polym. J.* **30**, 315 (1998)
- T.N.M. Cervantes, D.C. Bento, E.C.R. Maia, D.A.M. Zaia, E. Laureto, M.A.T. Da Silva, G.J. Moore, H. De Santana, *J. Mater. Sci.: Mater. Electron.* **23**, 1916 (2012)
- E.C.R. Maia, D.C. Bento, E. Laureto, D.A.M. Zaia, E.M. Thérézio, G.J. Moore, H. De Santana, *J. Serb. Chem. Soc.* **78**, 507 (2013)
- M.R.V. Lanza, R. Bertazzoli, *J. Appl. Electrochem.* **30**, 61 (2000)